4. STRUCTURE OF THE PERU FOREARC FROM MULTICHANNEL SEISMIC-REFLECTION DATA[1]

Gregory F. Moore[2] and Brian Taylor[3]

ABSTRACT

Multichannel seismic-reflection data collected on the Peru margin as part of Leg 112 of the Ocean Drilling Program predrilling site survey define some tectonic and sedimentary features of the Lima and Yaquina basins. A narrow accretionary prism is imaged at the toe of the trench slope in both areas. Landward of the accretionary prism is a transition zone that may be underlain by older accreted material and/or attenuated continental crust. Lima and Yaquina basins are underlain by disrupted reflectors that were interpreted as continental crust. The sedimentary section is characterized by lens-shaped seismic sequences that are cut by numerous, small-displacement, normal faults.

INTRODUCTION

As part of the predrilling site survey for Leg 112 of the Ocean Drilling Program, approximately 1550 km of 24-channel, seismic-reflection data were collected on the Peru margin by the Hawaii Institute of Geophysics (Fig. 1). During a 13-day cruise in March 1985, on board the *Moana Wave*, we concentrated on the trench and landward trench slope, which included the Lima and Yaquina basins (Kulm et al., 1982). Approximately 650 km of data was collected in the northern (Yaquina Basin) area (Fig. 2), and 895 km of data was collected in the southern (Lima Basin) area (Fig. 3). Here, we present several seismic-reflection sections from the Peru margin and offer preliminary interpretations. We limit our discussion to structural aspects of the seismic data and concentrate on the lower-slope region; stratigraphic aspects and upper-slope structures are addressed by Ballesteros et al. (this volume).

DATA ACQUISITION AND PROCESSING

The data were acquired with a 24-channel Western Geophysical hydrophone streamer. The 66 2/3-m group interval produced a 1600-m active array. Exactly 8 s of data was digitally recorded at a rate of 1 ms per sample using a Texas Instruments DFS-V in SEG-B format. Recording delays were used in deep water. Satellite navigation was recorded as position vs. time; thus, all processed seismic lines are annotated in time, rather than by CDP or shot-point number. Because we could not control velocity adequately for time-to-depth conversions, our discussion refers to depths in seconds of two-way traveltime rather than meters.

Our sound source consisted of air guns that were fired at 33 1/3-m intervals to yield 24-fold CDP coverage. A semi-tuned array of four air guns (120, 200, 300, and 500 in.^{3}) was used in the Yaquina Basin survey. Intermittent mechanical problems with the air guns forced us to fire various combinations of air guns during the Yaquina Basin survey. The resulting change in source signature degraded the quality of the data somewhat. We changed the air-gun towing system and used only two air guns (300 and 500 in.^{3}) for the Lima Basin survey. These guns were stable, so only minor source changes were needed in this part of the survey.

Data processing was conducted at the University of Tulsa with a VAX 11/750 using a Phoenix processing system (Seismograph Service Corp.) and consisted of the following steps:

1. Demultiplex and resample to 2 ms;
2. Edit noisy traces;
3. CDP sort and resample to 4 ms;
4. Analyze velocity at approximately 1-km intervals;
5. Deconvolution (predictive or spiking);
6. Apply NMO and stack;
7. Scale (500 ms Automatic Gain Control [AGC]);
8. Time-varying filter: 10, 15, 50, 55 Hz (to Water Bottom [WB] plus 600 ms); 5, 10, 40, 50 Hz (from WB plus 600 ms to WB plus 1100 ms); 5, 10, 30, 40 Hz (from WB plus 1100 ms to end of record);
9. Finite-Difference Migration of unscaled stacked section; and
10. Filter (10, 15, 50, 55 Hz) and scale (500 ms AGC).

Spiking deconvolution was applied to most of the data with varying success. The air-gun-bubble pulse obscures details of reflectors in many parts of the data.

Migration velocities were estimated from a combination of Multi-Channel Seismic (MCS) stacking velocities, Hawaii Institute of Geophysics (HIG) refraction velocities (Hussong and Wipperman, 1981), and migration-velocity analyses performed by von Huene and Miller (this volume). We also performed several migration-velocity tests on lines 5 and 14.

YAQUINA BASIN SEISMIC-REFLECTION DATA

Line 5 (Fig. 4 and Plate 1, back pocket) illustrates the major tectonic features of the Yaquina Basin region. The thin (approximately 100 m), hemipelagic, sediment cover on the Nazca Plate is onlapped by 350 to 400 ms of horizontally stratified trench sediment, forming a 3-km-wide trench. Seabeam bathymetric data across the trench in this area (Bourgois et al., 1986) show that the trench is relatively narrow where line 5 crosses it because of the impending subduction of one of the large ridges discovered by Kulm et al. (1973). Farther north, the trench is wider (greater than 5 km) and contains up to 750 ms of sediment where it is crossed by line 3 (Fig. 5). Sediment cores indicate that these trench sediments are silt and sand turbidites interlayered with mud (Kulm et al., 1981; Schweller et al., 1981).

Lines 3 and 5 (Fig. 5 and Plate 1) show that some trench sediment is presently being accreted to the base of the landward trench slope in packets bounded by landward-dipping thrust

[1] Suess, E., von Huene, R., et al., 1988. *Proc. ODP, Init. Repts.*, 112: College Station, TX (Ocean Drilling Program).

[2] Department of Geosciences, The University of Tulsa, Tulsa, OK 74104.
[3] Hawaii Institute of Geophysics, 2525 Correa Road, Honolulu, HI 96822.

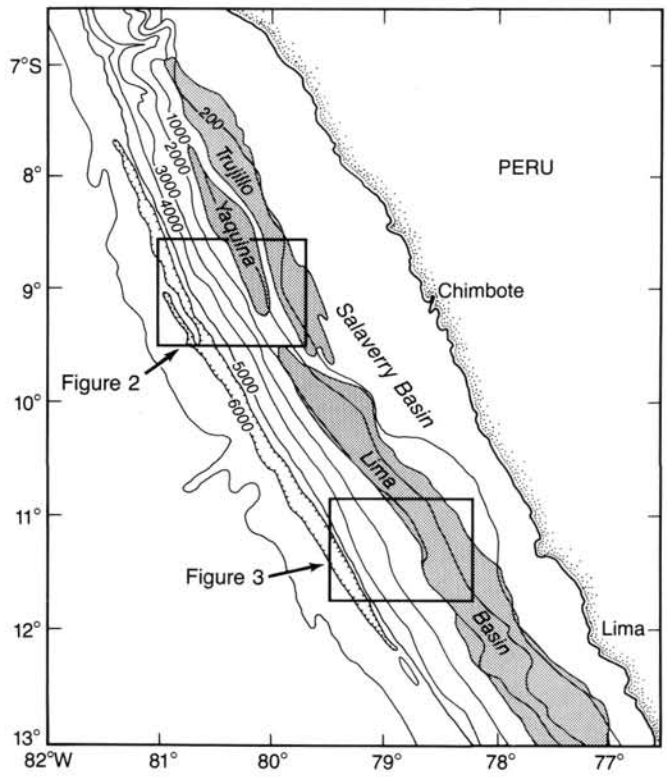

Figure 1. Regional tectonic map of the Peru offshore area showing location of study areas illustrated in Figures 2 and 3. Bathymetry from Thornburg and Kulm (1981).

faults. Incipient thrust faults are evident within the trench sediments at 1520 UTC on line 3. A landward-dipping decollement separates presently accreted packages from an underlying sedimentary sequence, approximately 400 ms thick on lines 3 and 5, which is subducted at least 6 km beneath the toe of the slope. The decollement on line 5 appears to ramp up to the surface above a fault in the ocean crust under the toe of the inner trench slope. Farther landward, the subducting sequence is not well imaged, and we cannot rule out the possibility that some of the sediments are underplated. The small volume of the accretionary prism and the length of time that subduction has been going on along this margin suggest that a large percentage of the trench sediments and all of the underlying oceanic pelagic sediments have been subducted. No sediment-filled graben is imaged in this part of the trench, indicating that sediment entrapment and subduction by graben is a much less important process than thought by Hilde (1983).

The top of the descending Nazca Plate can be traced at least 40 km beneath the landward trench slope on all of our seismic lines. Based on seismic refraction data, Kulm et al. (1981) estimated that the oceanic plate dips beneath the overriding plate at 10° to 15°. An accretionary prism, bounded below by the descending plate and characterized by internal landward-dipping reflectors (LDRs), is imaged on line 5 from 2140 UTC to at least 2300 UTC. The landward boundary of the prism is defined by a strong LDR that is best imaged on the reprocessed version of CDP-2 (von Huene et al., 1985).

A transition zone between the accretionary complex and the seaward edge of continental crust was interpreted on CDP-2 by von Huene et al. (1985). We correlate this transition zone with the lower-slope terrace located between 2320 UTC and approximately 0050 UTC on line 5. The sedimentary cover that lies on

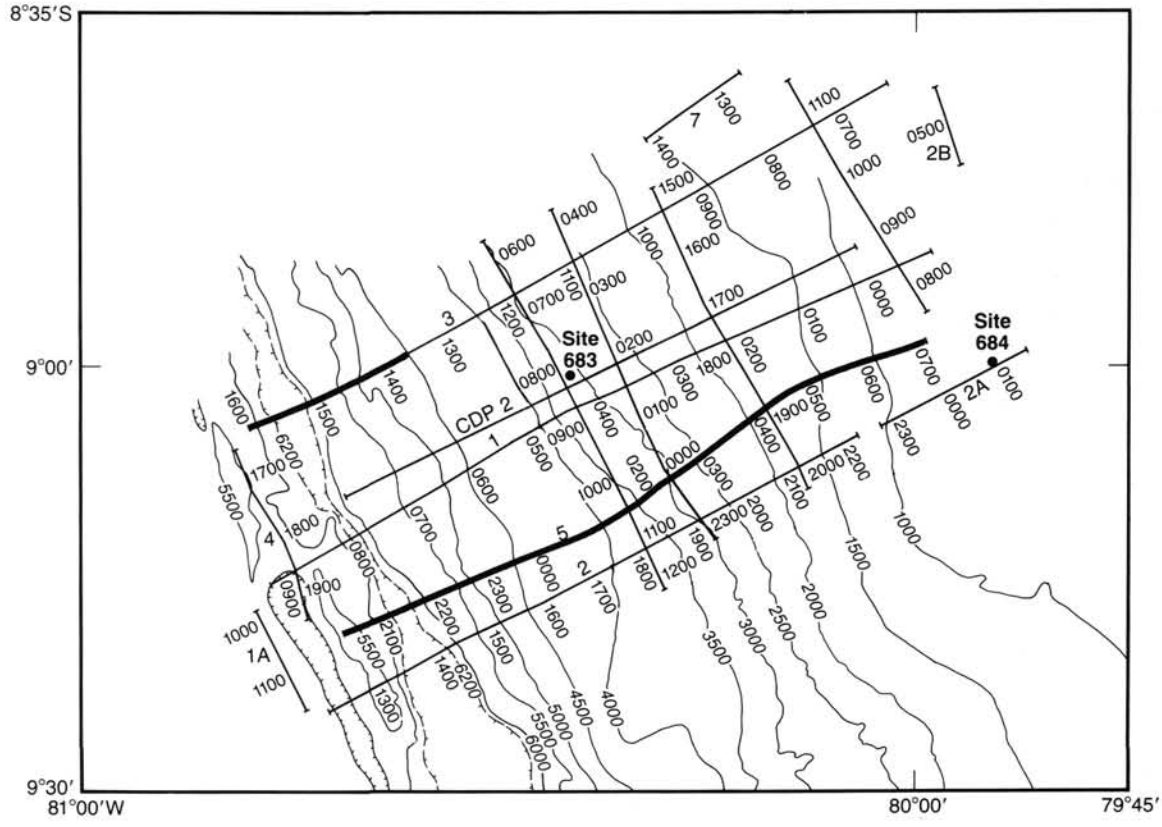

Figure 2. Track lines of MCS data acquisition in the Yaquina Basin area. Heavy lines indicate locations of seismic data illustrated in Figure 5 and Plate 1 (backpocket foldout).

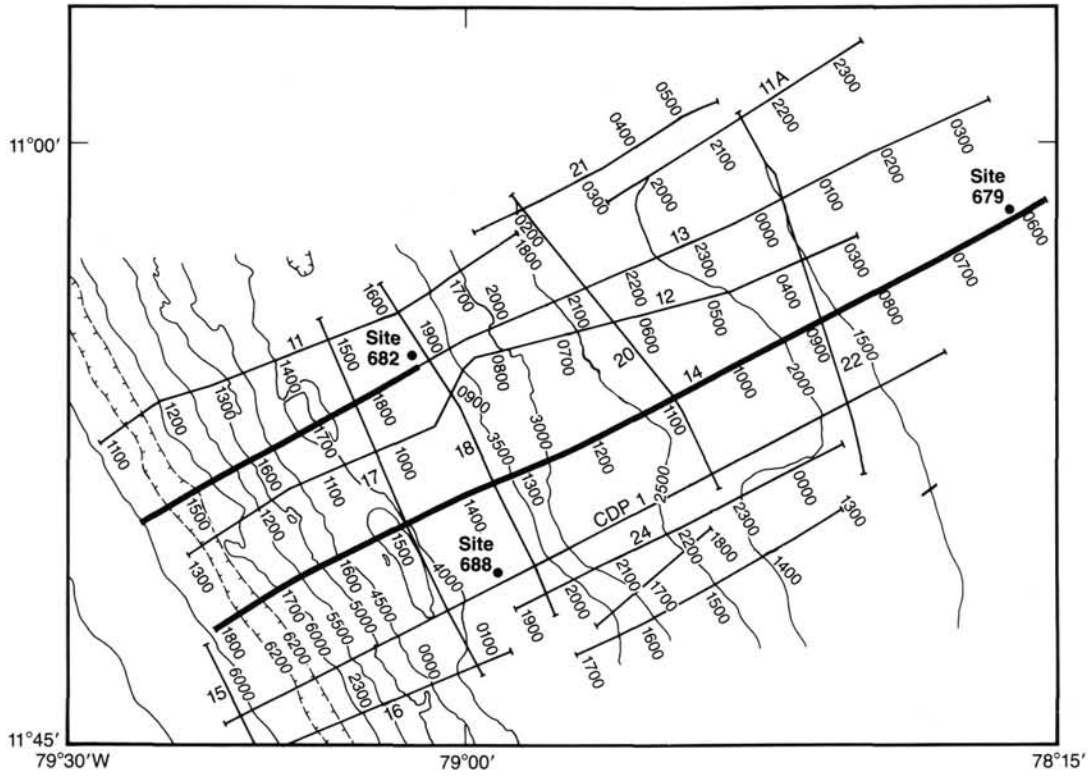

Figure 3. Track lines of MCS data acquisition in the Lima Basin area. Heavy lines indicate locations of seismic data illustrated in Figure 6 and Plate 1 (backpocket foldout).

top of this transitional crust is thin (approximately 500 ms), and the seismic signature of the crust is characterized by LDRs.

A strong, highly faulted reflector defines the interface between Neogene strata and underlying older strata on line 5 from 0050 UTC to its landward end. This reflector, at approximately 5.7 s at 0130 UTC, is identified as the top of the Eocene by Ballesteros et al. (this volume). This reflector is offset by seaward-dipping normal faults, and a large rotated block occurs between 0345 and 0405 UTC at a two-way traveltime of 4.5 to 4.7 s. Two landward-dipping normal faults downdrop the reflector at the eastern end of the seismic line. The overlying Neogene sequences are also cut by these normal faults, some of which reach the seafloor. Seismic line CDP-2, processed with prestacking migration by von Huene et al. (1985), images these normal faults clearly.

The Neogene sediment fill in Yaquina Basin has a maximum thickness of 2.0 s (approximately 1700–1800 m) near 0410 UTC. Ballesteros et al. (this volume) divided the Neogene strata into several seismic stratigraphic sequences and discussed the structural controls on their development.

LIMA BASIN SEISMIC-REFLECTION DATA

Line 14 (Fig. 4 and Plate 1) illustrates some of the major tectonic features of the Lima Basin section of the Peru forearc. Normal faults cut the Nazca Plate with its thin, hemipelagic sediment cover as it descends into the Peru Trench. The trench axis is approximately 2 km wide on line 14, but ranges up to 3 km wide on other Lima Basin seismic lines. A 400- to 500-m-thick wedge of trench fill sediments overlies and onlaps the underlying hemipelagic sediments. The horizontally stratified, laterally continuous nature of the trench strata suggests that these are turbidites.

As in the Yaquina area, the top of the subducting plate can be traced at least 40 km landward beyond the base of the slope. Although unambiguous interpretations of the structure of the plate are impossible on time sections, the record shows evidence for large-scale normal faults in the oceanic crust beneath the landward slope. An apparent subducting graben is imaged at 1625 UTC (Plate 1). Preliminary depth conversions suggest that the upward bend in the oceanic crust reflector at about 1450 UTC is a velocity pullup caused by the overlying high-velocity continental crust (see Hussong and Wipperman, 1981). The top of oceanic crust on line 13 (Fig. 6) shows much less topography than on line 14.

The lowermost trench slope is characterized by internal LDRs (Figs. 4 and 6). These LDRs were interpreted by Hussong et al. (1976) and Hussong and Wipperman (1981) as imbricate thrust planes. These scientists reported that the seismic velocity of this material was 3.5 km/s and suggested that it represents a small accretionary prism of offscraped oceanic plate and trench sediments, a suggestion with which we concur. The landward boundary of the prism is defined by a strong LDR on line 14 and is well displayed on CDP-1 (Hussong et al., 1976).

A transition zone between the accretionary complex and the seaward edge of the continental crust, located between 1620 and 1330 UTC on line 14 and between 1700 and 1900 UTC on line 13, defines a lower-slope terrace. This region is similar to the transition zone between continental crust and accretionary prism defined along the Middle America Trench off Mexico (Moore et al., 1982). A small sedimentary basin that lies on top of this transitional crust may be as much as 2 s (approximately 1800 m) thick. The basin sediments are disrupted by a landward-verging reverse fault and folds at the seaward edge of the basin on line 14. A near-vertical fault at the crest of an anticlinal structure offsets the seafloor topography in the middle of this basin on line 13. This faulted anticline is along strike from structures interpreted to be diapirs on high-exaggeration, single-channel, analog seismic records by Hussong and Taylor (1985). A prominent bottom-simulating reflector, probably caused by reflection from the base of a gas hydrate, is well imaged in the basin sediments but is less prominent in the accretionary prism.

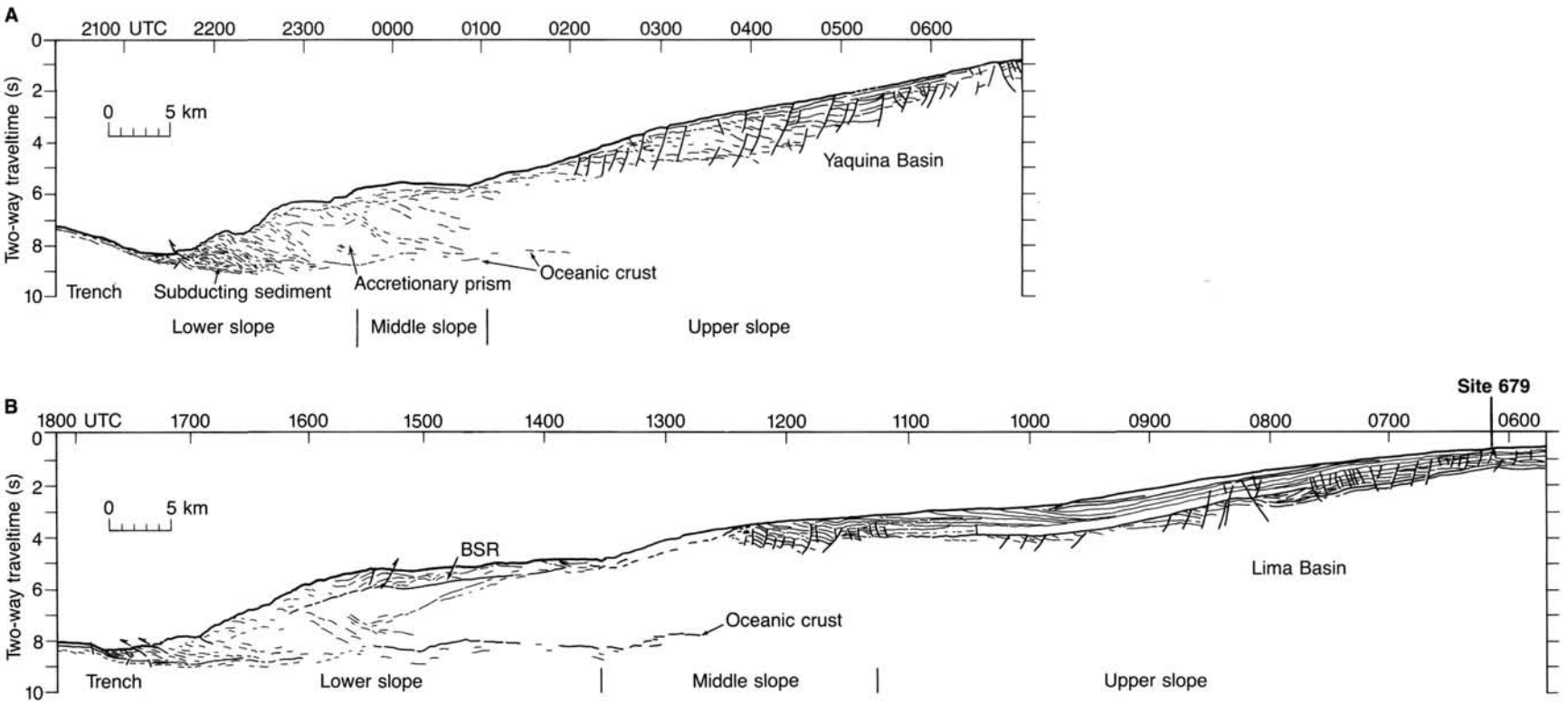

Figure 4. Interpretive line drawings of Peru seismic lines. Locations shown in Figures 2 and 3. Uninterpreted plots of seismic sections shown in Plate 1 (backpocket foldout). Locations of lower-, middle- and upper-slope regions from Bourgois et al. (1986) and von Huene et al. (1987).

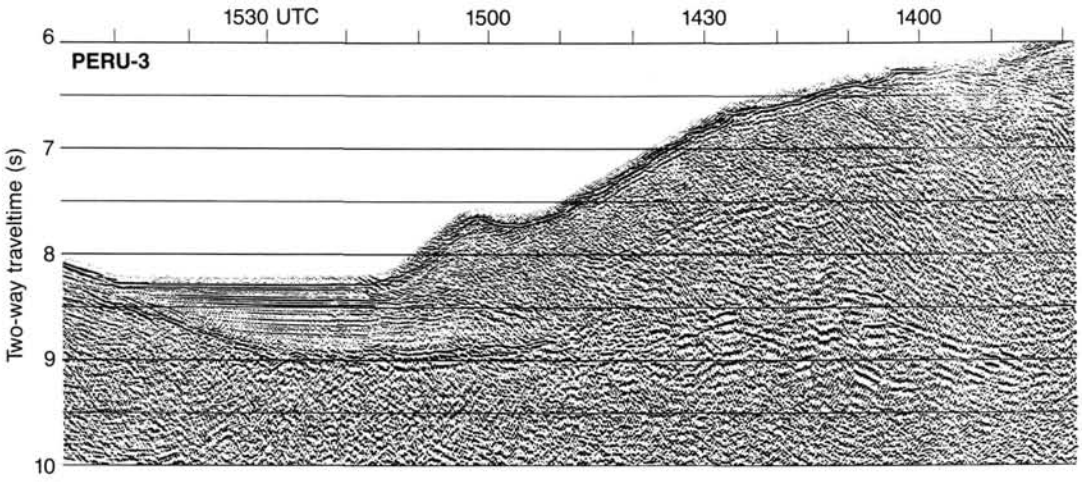

Figure 5. Enlarged portion of line 3 across toe of Peru Trench slope off Yaquina Basin.

The midslope region lies between approximately 1330 and 1130 UTC on line 14. The basement reflector in this region is poorly defined, and the overlying sedimentary section is strongly disrupted by several prominent seaward-dipping normal faults. These faults extend almost to the seafloor and separate large rotated blocks. Landward of 1130 UTC, a sharp reflector marks a regional angular unconformity between middle and upper Miocene strata. Under this unconformity, fault blocks contain up to 250 ms of post-Eocene sediment (e.g., 1005 UTC).

Approximately 1.3 s of Neogene strata overlie the Miocene unconformity (see Ballesteros et al., this volume). The section is characterized by parallel groups of reflectors bounded by unconformities. The unconformities are defined by basal onlap of the overlying sequence. Between the seafloor and 3.4 s, strata dip landward from about 0935 to 1020 UTC. This landward dip, attributed to relative uplift of the midslope region by Hussong and Wipperman (1981), may be due to contourite deposition (see Ballesteros et al., this volume).

A broad basement high is evident in the deep subsurface between 0805 and 0825 UTC. Sediments above this structure are also cut by numerous small-scale faults. Landward of this structure, the shallow sedimentary section is cut by a series of normal faults. Most faults dip landward from 0800 to 0705 UTC, and most faults dip seaward from 0705 UTC to the end of the line where Site 679 was drilled.

DISCUSSION

The basic structure of the Lima and Yaquina survey areas is similar, but some important differences do occur. Both areas have a narrow accretionary prism at the base of the landward trench slope. Only about one-third of the trench sediments are accreted; the remainder are subducted beyond the toe of the slope. A transition zone of older accreted sediments or attenuated continental crust occurs between the accretionary prism and the well-defined continental crust landward. The Yaquina Basin area is much more highly faulted, and thus the sedimentary sequences are much less subject to interpretation (see Ballesteros et al., this volume). Normal faults cutting the upper slopes of both regions indicate an extensional regime in the continental crust landward of the accretionary prism.

ACKNOWLEDGMENTS

We thank John Weigant, Abera Retta, Steve Ruppert, Maria Silva, Robert Horine, and Todd Jimeson for their help in processing the seismic data. Steve Ruppert and Mark Ballesteros collaborated on the seismic interpretations. Reviews by Roland von Huene and Mark Ballesteros helped to improve the manuscript. This work was funded by JOI and USSAC.

REFERENCES

Bourgois, J., Pautot, G., Bandy, W., Boinet, T., Chotin, P., Huchon, P., Mercier de Lepinay, B., Monge, F., Monlau, J., Pelletier, B., Sosson, M., and von Huene, R., 1986. Regime tectonique de la marge andine convergente du Perou (Campagne SEAPERC du N.O. *Jean-Charcot*, juillet 1986). *C. R. Acad. Sci. Paris*, 303:1599–1604.

Hilde, T.W.C., 1983. Sediment subduction versus accretion around the Pacific. *Tectonophysics*, 99:381–397.

Hussong, D. M., Edwards, P. B., Johnson, S. H., Campbell, J. F., and Sutton, G. H., 1976. Crustal structure of the Peru–Chile Trench: 8°S to 12°S latitude. *Am. Geophys. Union, Mono.*, 19:71–86.

Hussong, D. M., and Taylor, B., 1985. Peru forearc structure and tectonic disruption. *Eos, Trans. Am. Geophys. Union*, 66:1105.

Hussong, D. M., and Wipperman, L. K., 1981. Vertical movement and tectonic erosion of the continental wall of the Peru–Chile Trench near 11°30′S latitude. *Geol. Soc. Am. Mem.*, 154:509–524.

Kulm, L. D., et al., 1973. Tholeiitic basalt ridge in the Peru Trench. *Geology*, 1:11–14.

Kulm, L. D., Prince, R. A., French, W., Johnson, S., and Masias, A., 1981. Crustal structure and tectonics of the central Peru continental margin and trench. *Geol. Soc. Am. Mem.*, 154:445–468.

Kulm, L. D., Resig, J. M., Thornburg, T. M., and Schrader, H. J., 1982. Cenozoic structure, stratigraphy and tectonics of the central Peru forearc. *Geol. Soc. London Spec. Publ.*, 10:151–170.

Moore, J. C., Watkins, J. S., Shipley, T. H., McMillen, K. J., Bachman, S. B., and Lundberg, N., 1982. Geology and tectonic evolution of a juvenile accretionary terrane along a truncated convergent margin: synthesis of results from Leg 66 of the Deep Sea Drilling Project, southern Mexico. *Geol. Soc. Am. Bull.*, 93:847–861.

Schweller, W. J., Kulm, L. D., and Prince, R. A., 1981. Tectonics, structure, and sedimentary framework of the Peru–Chile Trench. *Geol. Soc. Am. Mem.*, 154:323–349.

Seely, D. R., Vail, P. R., and Walton, G. G., 1974. Trench slope model. *In* Burk, C. A., and Drake, C. L. (Eds.), *The Geology of Continental Margins*: Berlin-Heidelberg (Springer-Verlag), 249–260.

Thornburg, T. M., 1985. Seismic stratigraphy of Peru forearc basins. *In* Hussong, D. M., et al. (Eds.), *Atlas of the Ocean Margin Drilling Program, Peru Continental Margin, Region VI*: Woods Hole (Marine Science International).

Thornburg, T. M., and Kulm, L. D., 1981. Sedimentary basins of the Peru continental margin: structure, stratigraphy, and Cenozoic tectonics from 6°S to 16°S latitude. *Geol. Soc. Am. Mem.*, 154:469–508.

von Huene, R., Kulm, L. D., and Miller, J., 1985. Structure of the frontal part of the Andean convergent margin. *J. Geophys. Res.*, 90: 5429–5442.

von Huene, R., Suess, E., Emeis, K., and Leg 112 Shipboard Scientific Party, 1987. Convergent tectonics and coastal upwelling: a history of the Peru continental margin. *Episodes*, 10:87–93.

Ms 112A-121

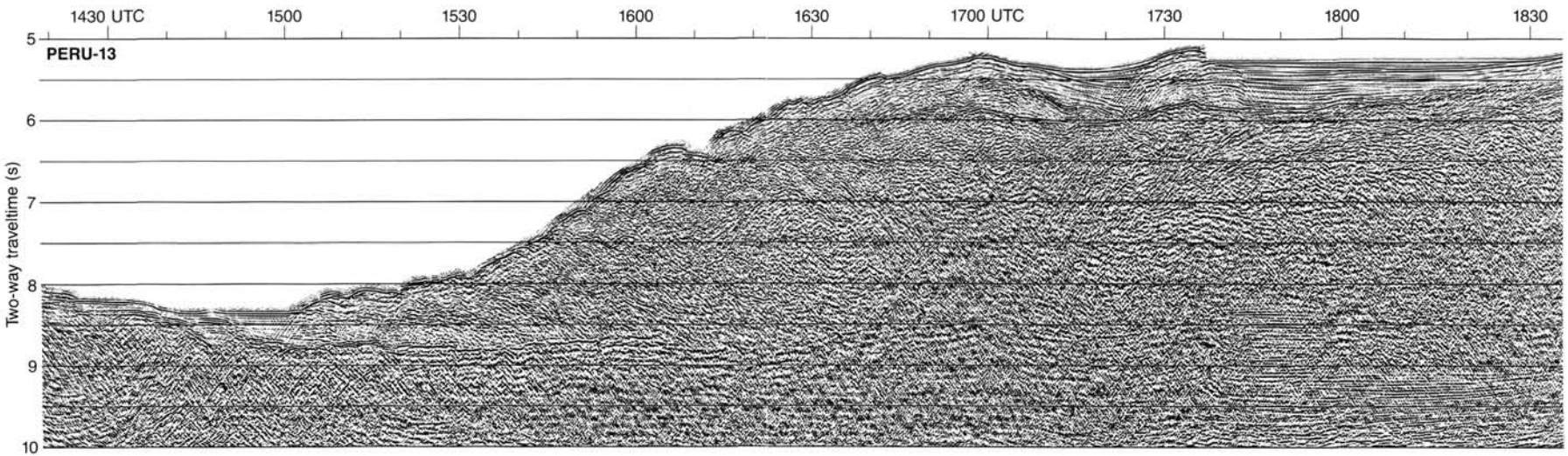

Figure 6. Enlarged portion of line 13 across toe of trench slope off Lima Basin. Note the well-developed BSR.